

Ultrafast X-ray Absorption Spectroscopy using Laser-Driven Electron X-ray Sources (LEXS)

Guangjun Cheng, Fang Shan, Abhi Freyer, and Ting Guo*

Department of Chemistry, University of California, One Shields Avenue, Davis, CA 95616

ABSTRACT

A laser driven electron x-ray source (LEXS) using a high repetition rate, terawatt laser system is described. The laser system has adopted design features that make it more suitable for the generation of hard x-ray pulses. These features include a simplified pumping scheme to reduce cost and complexity, a $\lambda/4$ broadband regenerative amplifier to support high-energy, short optical pulse generation, and a 50-Hz repetition rate to achieve both a desired pulse energy and a simple compressor design. Preliminary results on x-ray generation using this system are reported. A new method, ultrafast selected energy x-ray absorption spectroscopy (USEXAS), based on this LEXS is discussed.

Keywords: ultrafast x-rays, x-ray absorption spectroscopy, terawatt lasers, ultrafast reaction dynamics, atomic motion

1. INTRODUCTION

The advancing high power laser technologies have improved our ability of building more compact sized terawatt lasers¹⁻³. These lasers have made it easier to implement a special type of x-ray sources, the laser-driven electron x-ray source (LEXS)⁴⁻⁶. The development of LEXS runs a parallel path with the development of laser-plasma x-ray sources for plasma and fluid diagnosis. The latter has been studied for over three decades, and has been reviewed in many excellent articles^{7,8}. Recently, elaborate schemes have been used to produce ultrafast hard x-ray pulses of hundreds of femtoseconds⁹⁻¹³, and various diffraction measurements have been performed with these sources, including LEXS^{5,6,14,15}.

A LEXS consists of two major components, a terawatt laser system and an x-ray target apparatus. A terawatt laser is necessary for generating energetic electrons (a few keV to a few hundred keV) of subpicosecond pulse length, and special targets are needed for the generation of desired x-ray wavelengths and long operation hours for x-ray absorption measurements. We will present the results of our design and characterization of these two components. In this article, we will also discuss a specific method in which LEXS is used for studying x-ray absorption spectroscopy.

X-ray absorption spectroscopy (XAS), which includes both extended x-ray absorption fine structure (EXAFS) and x-ray absorption near edge spectroscopy (XANES), has been used to obtain structures of amorphous and crystalline materials

for many decades¹⁶. EXAFS is now a well-established method because of the straightforward relationship between the modulation in the absorption spectrum and the interatomic distances, coordination numbers, and distance disorders. EXAFS mainly relies on photoelectrons with kinetic energies over 50 eV. It is thus generally accepted that the pattern of EXAFS is largely determined by the atomic configuration of the material studied. Theories of EXAFS have already extended into the ultrafast region¹⁷. On the other hand, XANES is more sensitive to small changes in atomic and electronic configurations, although XANES is more difficult to interpret. The range of energies of the photoelectrons influencing XANES includes two regions, pre- (between a few eV below and above the edge) and near edge (from the edge to ~ 50 eV above the edge). Therefore, both EXAFS and XANES are useful for understanding reactions by revealing the dynamics of atomic and electronic motions.

There are several distinctive advantages of using LEXS to investigate atomic motion by scrutinizing the changes in x-ray absorption spectra during reactions. First, if it is possible to monitor the spectrum in both the pre/near edge and the extended regions, one can separate electronic motion from atomic motion. Second, XAS on the ultrafast time scale should be self-referenced, i.e., only the net change occurring to the static structure, i.e., the dynamic absorption spectrum, is needed for interpretation. The static structure can be studied and interpreted separately.

Although broadband x-ray pulses can be produced with LEXS by processes such as Bremsstrahlung radiation or through other processes such as plasma (Stark) broadening from thermal sources, it is important to realize that these broadband sources are usually unlikely to cover the energy range or the equivalent reciprocal space needed for an accurate Fourier Transformation. For example, a bandwidth of several hundred to over a thousand eV is needed for Fourier transforming an EXAFS pattern in the multiple keV energy range into the real space. On the other hand, Bremsstrahlung radiation is two to three orders of magnitude weaker than the characteristic emission, and data acquisition times become a concern when the former is used for absorption measurements. Therefore, the advantage of using LEXS in x-ray absorption spectroscopy lies in the use of intense characteristic emission that covers important spectral regions in which the temporal evolutions of the absorption spectrum can help us gain understanding of reaction dynamics.

In the following, we will address the laser system first, followed by the description of the x-ray target apparatus. The new method, USEXAS, will be discussed in Section 4.

2. TERAWATT LASER SYSTEM

Ultrafast terawatt lasers¹⁸⁻²² have become important tools to researchers in many areas, including ultrafast x-ray diffraction and absorption spectroscopy^{5,6,11,23}. To make these lasers more versatile and affordable to more users, a balance among several parameters, including the repetition rate, energy per pulse, pulse-duration, and spectral profile, must be achieved. For these lasers to be used in LEXS⁴, for instance, laser pulses are preferred to have energies on the order of 50 mJ/pulse so that x-ray spot sizes can be made small while the conversion efficiency from laser photons to hard x-rays remains high. In addition, no cumbersome accessories such as vacuum compressors should be used. Other important criteria are that the size of the system be compact, and that the cost be affordable. A direct conclusion from these requirements is that the highest possible repetition rate should be used whenever possible, which is usually determined by the availability of pump lasers.

The laser described here has achieved this balance. The repetition rate, pulse energy, and pulse duration have been optimized for an easy implementation and for various applications such as LEXS. The highest pulse energy and the shortest pulse duration are determined by the applications and the pump lasers, although the B-integral of the air should also be taken into account. For example, if the beam path length between the compressor and the user-end instruments is less than a few meters, then a 2-W, 30-mm diameter ($1/e^2$) beam made of pulses of 40-fs duration, 50 mJ/pulse at a 50-

Hz repetition rate will not be seriously distorted. On the other hand, pulses from a 10-Hz laser with the same average power (200 mJ/pulse) and other parameters will be severely distorted, and a vacuum compressor and beam delivery line would have to be used.

The chirped-pulse-amplification (CPA) ²⁴ Ti: Sapphire laser system is shown in Figure 1. The homemade oscillator has a bandwidth of over 100 nm, and folding mirrors are low group velocity delay mirrors (LGVD, CVI). Based on our dispersion calculations for a 4-mm Brewster-cut Ti: Sapphire crystal, the separation of the compensating prism pair is 59 cm. The pump laser is a frequency doubled Nd:YAG laser (Millennia Vs, Spectra-Physics). This pump laser possesses a high beam pointing stability despite its short cavity length. The pulses from the oscillator are measured using a scanning interferometric autocorrelator with a diode detector. The scanning arm of the autocorrelator is driven by a piezo oscillating at 4 Hz (MDT691, Thorlabs). Measurements are done together with an external prism pair, which compensate the pulse broadening produced by external cavity optics.

A typical spectrum from the mode-locked oscillator at 2-W pump energy is over 110 nm. The autocorrelation trace of the oscillator has been obtained with the scanning autocorrelator, and the pulse duration is measured to be 15 ± 1 fs. The average power of the oscillator is ~100 mW.

The output from the oscillator is sent into an all-reflective optics, large bandwidth expander ²⁵. This expander has a bandwidth of over 130 nm ^{3,25}, and the stretching factor is ~ 100,000. In order to reduce the feedback from the regenerative amplifier, a lens tissue is placed between the expander and the regenerative amplifier. This effectively reduces the feedback while it still lets enough light into the regenerative amplifier.

The Ti: Sapphire crystal in the regenerative amplifier is pumped by a beam with 20% of the output energy from a 50-Hz pump laser (Continuum, 9050 Precision). The pumping energy can be further adjusted with a waveplate-polarizer combination, and the operation energy is between 3 to 4 W. The seeding pulse passes through a thin-film-polarizer (TFP), and a $\lambda/2$ waveplate and a Faraday rotator. A $\lambda/4$ Pockels cell (PC) is employed. The PC is triggered by the AND signal of a 50-Hz master clock that is used to trigger the pump laser, and the oscillator pulse train. This arrangement assures that no injection occurs when the oscillator drops out of mode-locking. A jitter of ~ 8 ns between these two pulse trains exists. However, this jitter is small compared with the 80-ns time delay between the seeding and pump pulses. The number of round trips is 14. The gain-narrowing problem is overcome by an insertion of a thin pellicle (1.8 μm at a 25-degree angle of incidence) in the regenerative amplifier.

One of the drawbacks of using a $\lambda/4$ PC originates from the fact that regular pulse generators are unable to lower the voltage to zero in a short time (a few nanoseconds). The LASERMATRIX PC uses solid-state devices to ensure fast rise and fall times. The rising and falling times of the PC are both 4 ns. The other drawback of a $\lambda/4$ regenerative amplifier is that different static rotations or losses are introduced for different wavelengths in the spectrum. This becomes worse for pulses with a wide spectrum. However, this problem is less a factor in our case because the spectral shaping by the pellicle is used: the pellicle not only counters gain-narrowing, but also balances the losses caused by other intracavity elements such as the waveplate and the PC.

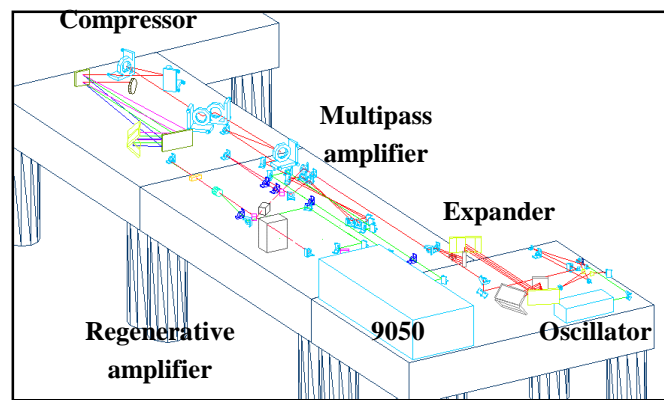


Figure 1. Schematic of UC Davis terawatt laser system.

The spectral width from the regenerative amplifier is over 80 nm. The spectral profiles are similar with or without the seeding from the oscillator, although the pump energy is reduced when the regenerative amplifier is seeded. At 3-W pumping pulse energy, a 3-mJ/pulse output is obtained. The diameter of the output from the regenerative amplifier is ~ 1mm.

The collimated output from the regenerative amplifier is then sent into the multipass amplifier (see Figure 1). Relay imaging systems using only one lens are adopted, and a flattop pump beam-profile of 5-mm diameter is obtained at the multipass Ti: Sapphire crystal. The crystal is pumped by the two beams from the 50-Hz laser with a total energy of over 400 mJ/pulse. After this amplifier, the 3-mJ output from the regenerative amplifier is amplified to 120 mJ. This corresponds to 30% conversion efficiency. The FWHM of the final pulse after compression is 38 fs after grating angles and separation have been optimized, and the pulse energy is 55 mJ/pulse.

3. X-RAY TARGET APPARATUS

A wire x-ray target without any moving fixtures near the laser focus has been designed. The schematic of the target apparatus is shown in Figure 2. This apparatus is similar to another wire apparatus reported in the literature, except the stability of the current one is much higher because of the no moving-fixture design⁴. In brief, the terawatt laser beam is focused by a metallic parabolic mirror onto a moving metal wire which slides in a spiral groove cut on a Teflon rod. The wire, coming off a spool which contains a 1000-meter wire, is pressed by a presser and pulled through the laser focus by a puller located outside the chamber (shaded rectangular box). The pulling speed is at 1.5 mm/sec. A Mylar film (SPEX, 80 mm wide, 3 μm thick) is used to protect the parabolic mirror. X-ray spectrometer consists of a GaAs single crystal (111) and a LN₂ cooled CCD (deep depletion PI-LCX 576, Roper Scientific) detector.

We have observed broad diffraction patterns under similar conditions as we acquire the sharp line radiation $K_{\alpha 1}$ and $K_{\alpha 2}$ of copper, shown in Figure 3. The main difference is that the spot sizes are drastically different. Using shadowgraphy, a 25-μm spot size (for lines shown in Figure 3a) is found for the line emission and 180-μm for the broad diffraction line (as shown in Figure 3b). Since the focusing conditions are different in these two cases, it is believed that the broad diffraction line (Figure 3b) results from the large x-ray emission size, although spectral broadening is also possible. The results of the size measurements are shown in Figure 4. The left panel

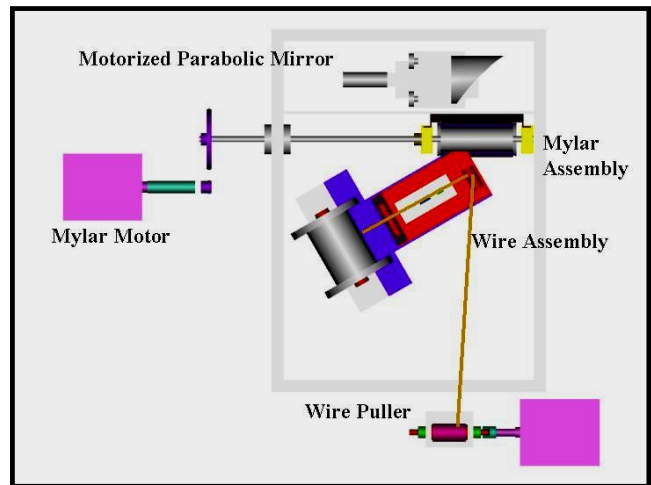


Figure 2. Target apparatus in the LEXS.

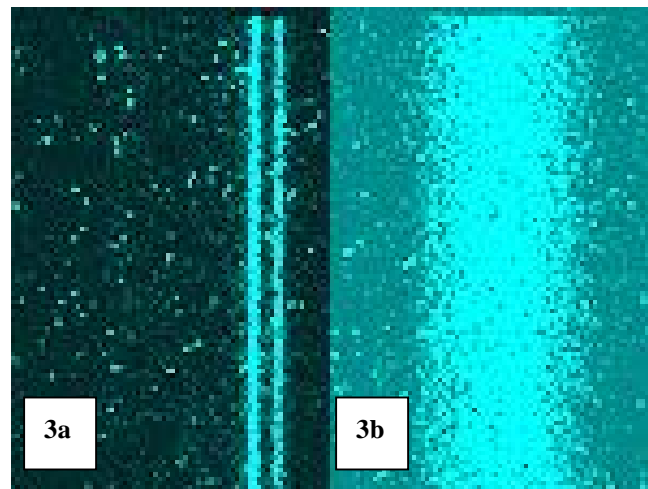


Figure 3. Sharp (3a) and broad (3b) diffraction patterns from the same target (Cu) under different focusing conditions. The left panel (3a) is obtained with a sharp focus and has a much high flux than that of the right, which is emitted from a much larger spot.

corresponds to Figure 3a, the right to Figure 3b.

4. USEXAS

In order to use LEXS for structural investigation, new methodologies have to be developed. In this section, we will discuss a new x-ray absorption method, ultrafast selected energy x-ray absorption spectroscopy, or USEXAS. The aim is to extend our detection ability into visualizing atomic motion *during* ultrafast chemical and biological reactions by examining the interplay of electronic and atomic motions.

In USEXAS, two or more regions of the absorption spectrum in both the pre/near edge and the extended regions are monitored simultaneously and on the ultrafast timescale. For example, based on the discussion in Section 1, one can conclude that the absorption spectra in the extended region should remain the same during pure electronic motions. Therefore, if both the pre/near and the extended regions are monitored, we will be able to differentiate atomic motion from electronic motion. USEXAS can be implemented with characteristic x-ray emission lines, as demonstrated below.

Since USEXAS relies on a match between the emission lines of certain elements and the absorption edge of the interested elements, it is worth pointing out that it is not a method that can be applied to studying every element. Even so, the elements that can be studied with USEXAS all possess interesting ultrafast reaction dynamics. For example, Cs and Ru can be studied with the characteristic lines from Pb and Pr. Ni complexes can be investigated by line emission from W. Furthermore, Bremsstrahlung radiation from LEXS can be used to study other elements, although data acquisition times can be significantly longer.

A specific example, the photodissociation dynamics of the axial ligands in complexed Ni porphyrins, is used to illustrate the principle of this method. The Ni system has been used to mimic metalloproteins, and nanosecond x-ray absorption measurements have been

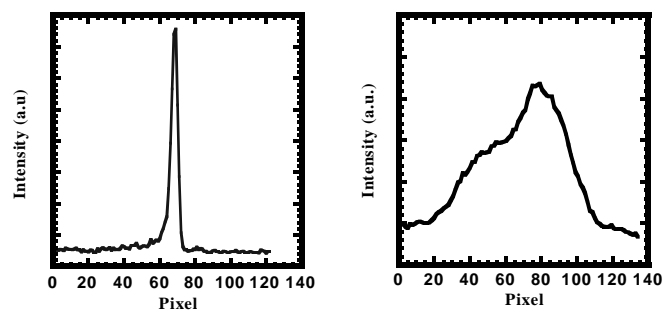


Figure 4. Spot size measurements of broad and sharp diffraction patterns. The size of the pixel is 22 μm .

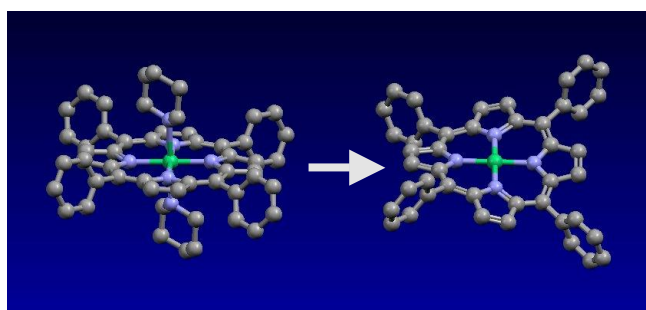


Figure 5. Dissociation of NiTPP bipiperidine (left) to NiTPP (right).

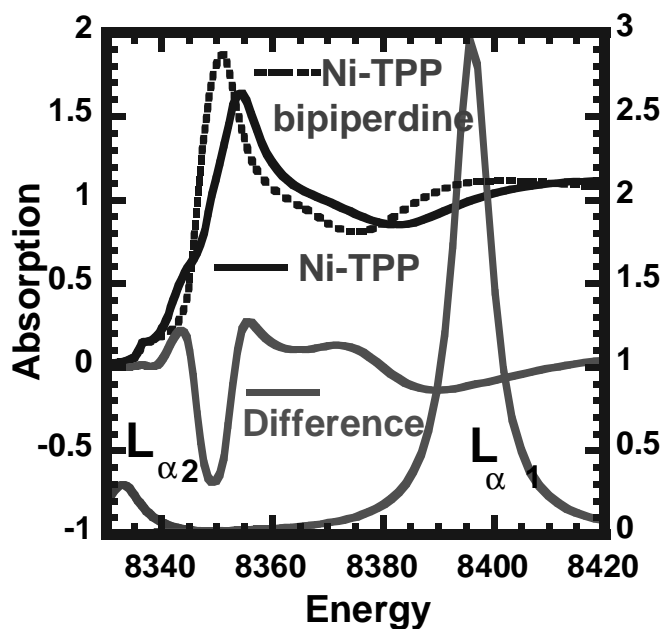


Figure 6. FEFF calculations of XAS patterns of NiTPP bipiperidine and NiTPP. Also shown are the $L_{\alpha 1}$ and $L_{\alpha 2}$ lines of W.

performed on this system²⁶. The structure of a tetraphenylporphyrin Nickel (NiTPP) with two axial piperidine ligands is shown in the left panel of Figure 5. The right panel shows NiTPP without these two ligands. We can use $L_{\alpha 1}$ and $L_{\alpha 2}$ of tungsten to probe the K edge of Ni in order to study this photochemical reaction.

Using FEFF 8.0 program²⁷⁻²⁹, we have calculated the XAS patterns in the regions covered by these two L lines. In this example, the patterns are drastically different for the complexed and dissociated NiTPP, as shown in Figure 6. We have to point out that although these calculations may resemble the real spectra, the position of the pre-edge peak corresponding to the 1s-4p (3d) transitions is obviously displaced from the one shown in the static measurements²⁶. In order to truthfully reproduce these spectra, higher levels of calculations may be needed³⁰.

5. CONCLUSION

We have demonstrated a cost-effective terawatt laser system that can be used to drive a LEXS. By taking advantage of the features of LEXS, we have proposed to use a new method, USEXAS, to study atomic motion during ultrafast reactions.

ACKNOWLEDGEMENTS

The authors thank Brad Lormand, Amy Neurauter, and El-Sayed Hassanein for their experimental assistance. This work is supported by a start-up fund at University of California, Davis, and the Camille and Henry Dreyfus New Faculty Awards Program. Acknowledgement is made to the Donors of The Petroleum Research Fund, administered by the American Chemical Society. TG is also grateful for the support of a summer faculty fellowship at University of California, Davis.

REFERENCES

- ¹ G. Cheng, F. Shan, A. Freyer, and T. Guo, "Compact 50-Hz Terawatt Laser for X-ray and Optical Spectroscopy," *Applied Optics*, Submitted, (2001).
- ² C. Leblanc, G. Grillon, J. P. Chambaret, A. Migus, and A. Antonetti, "Compact and Efficient Multipass Ti-Sapphire System For Femtosecond Chirped-Pulse Amplification At the Terawatt Level," *Optics Letters* **18**, 140 (1993).
- ³ C. P. J. Barty, T. Guo, C. Leblanc, F. Raksi, C. Rose-Petruck, J. Squier, K. R. Wilson, V. V. Yakovlev, and K. Yamakawa, "Generation of 18-Fs, Multiterawatt Pulses By Regenerative Pulse Shaping and Chirped-Pulse Amplification," *Optics Letters* **21**, 668 (1996).
- ⁴ T. Guo, C. Spielmann, B. C. Walker, and C. P. J. Barty, "Generation of hard x rays by ultrafast terawatt lasers," *Review of Scientific Instruments* **72**, 41 (2001).
- ⁵ C. Rischel, A. Rousse, I. Uschmann, P. A. Albouy, J. P. Geindre, P. Audebert, J. C. Gauthier, E. Forster, J. L. Martin, and A. Antonetti, "Femtosecond time-resolved X-ray diffraction from laser-heated organic films," *Nature* **390**, 490 (1997).
- ⁶ C. Rose-Petruck, R. Jimenez, T. Guo, A. Cavalleri, C. W. Siders, F. Raksi, J. A. Squier, B. C. Walker, K. R. Wilson, and C. P. J. Barty, "Picosecond-milliangstrom lattice dynamics measured by ultrafast X-ray diffraction," *Nature* **398**, 310 (1999).
- ⁷ M. H. Key and R. J. Hutcheon, "Spectroscopy of Laser Produced Plasmas," *Adv. At. Mol. Opt. Phys.* **16**, 201 (1980).
- ⁸ A. A. Hauer and G. A. Kyrala, "Laser-Plasma X-ray Emission: Its Creation, Diagnosis, and Applications in Transient Diffraction," in *Time-Resolved Diffraction*, edited by J.R Helliwell and P.M. Rentzepis (Clarendon Press; Oxford University Press, Oxford New York, 1997), pp. 71.
- ⁹ J. D. Kmetec, C. L. Gordon, J. J. Macklin, B. E. Lemoff, G. S. Brown, and S. E. Harris, "MeV X-Ray Generation With a Femtosecond Laser," *Physical Review Letters* **68**, 1527 (1992).
- ¹⁰ A. Rousse, P. Audebert, J. P. Geindre, F. Fallies, J. C. Gauthier, A. Mysyrowicz, G. Grillon, and A. Antonetti, "Efficient K Alpha X-Ray Source From Femtosecond Laser-Produced Plasmas," *Physical Review E* **50**, 2200 (1994).

- 11 R. W. Schoenlein, S. Chattopadhyay, H. H. W. Chong, T. E. Glover, P. A. Heimann, C. V. Shank, A. A. Zholents, and M. S. Zolotarev, "Generation of femtosecond pulses of synchrotron radiation," *Science* **287**, 2237 (2000).
- 12 I. V. Tomov, D. A. Oulianov, P. L. Chen, and P. M. Rentzepis, "Ultrafast time-resolved transient structures of solids and liquids studied by means of X-ray diffraction and EXAFS," *Journal of Physical Chemistry B* **103**, 7081 (1999).
- 13 J. Larsson, P. A. Heimann, A. M. Lindenberg, P. J. Schuck, P. H. Bucksbaum, R. W. Lee, H. A. Padmore, J. S. Wark, and R. W. Falcone, "Ultrafast structural changes measured by time-resolved X-ray diffraction," *Applied Physics a-Materials Science & Processing* **66**, 587 (1998).
- 14 T. Guo, Rose-Petruck, C., Jimenez, R., Raski, F., Squier, J., Walker, B.C., Wilson, K.R., Barty, C.P.J., SPIE, San Diego, **3157**, 84 (1997).
- 15 A. Rousse, C. Rischel, S. Fourmaux, I. Uschmann, S. Sebban, G. Grillon, P. Balcou, E. Foster, J. P. Geindre, P. Audebert, J. C. Gauthier, and D. Hulin, "Non-thermal melting in semiconductors measured at femtosecond resolution," *Nature* **410**, 65 (2001).
- 16 D. C. Koningsberger and R. Prins, X-ray absorption : principles, applications, techniques of EXAFS, SEXAFS, and XANES (Wiley, New York, 1988).
- 17 F. L. H. Brown, K. R. Wilson, and J. S. Cao, "Ultrafast extended x-ray absorption fine structure (EXAFS) - theoretical considerations," *Journal of Chemical Physics* **111**, 6238 (1999).
- 18 S. Backus, C. G. Durfee, M. M. Murnane, and H. C. Kapteyn, "High power ultrafast lasers," *Review of Scientific Instruments* **69**, 1207 (1998).
- 19 M. D. Perry and G. Mourou, "Terawatt to Petawatt Subpicosecond Lasers," *Science* **264**, 917 (1994).
- 20 A. Sullivan, H. Hamster, H. C. Kapteyn, S. Gordon, W. White, H. Nathel, R. J. Blair, and R. W. Falcone, "Multiterawatt, 100-Fs Laser," *Optics Letters* **16**, 1406 (1991).
- 21 Y. Beaudoin, C. Y. Chien, J. S. Coe, J. L. Tapie, and G. Mourou, "Ultrahigh-Contrast Ti-Sapphire Nd-Glass Terawatt Laser System," *Optics Letters* **17**, 865 (1992).
- 22 W. E. White, J. R. Hunter, L. Vanwoerkom, T. Ditmire, and M. D. Perry, "120-Fs Terawatt Ti-Al₂O₃/Cr-Lisralf6 Laser System," *Optics Letters* **17**, 1067 (1992).
- 23 F. Raksi, K. R. Wilson, Z. M. Jiang, A. Ikhlef, C. Y. Cote, and J. C. Kieffer, "Ultrafast X-Ray Absorption Probing of a Chemical Reaction," *Journal of Chemical Physics* **104**, 6066 (1996).
- 24 D. Strickland and G. Mourou, "Compression of Amplified Chirped Optical Pulses," *Opt. Commun.* **56**, 216 (1985).
- 25 B. E. Lemoff and C. P. J. Barty, "Quintic-Phase-Limited, Spatially Uniform Expansion and Recompression of Ultrashort Optical Pulses," *Optics Letters* **18**, 1651 (1993).
- 26 L. X. Chen, W. J. H. Jager, G. Jennings, D. J. Gosztola, A. Munkholm, and J. P. Hessler, "Capturing a photoexcited molecular structure through time-domain X-ray absorption fine structure," *Science* **292**, 262 (2001).
- 27 J. J. Rehr, A. Ankudinov, and S. I. Zabinsky, "New developments in NEXAFS/EXAFS theory," *Catalysis Today* **39**, 263 (1998).
- 28 J. J. Rehr, "Multiple-Scattering Approach to Surface Exafs - Theory Versus Experiment," *Surface Review and Letters* **2**, 63 (1995).
- 29 A. L. Ankudinov, B. Ravel, J. J. Rehr, and S. D. Conradson, "Real-space multiple-scattering calculation and interpretation of x-ray-absorption near-edge structure," *Physical Review B-Condensed Matter* **58**, 7565 (1998).
- 30 Y. Luo, H. Agren, M. Keil, R. Friedlein, and W. R. Salaneck, "A theoretical investigation of the near-edge X-ray absorption spectrum of hexa-peri-hexabenzocoronene," *Chemical Physics Letters* **337**, 176 (2001).